Discrete and Continuous Dynamical Systems - Series B
Vol. 38, 2026, pp. 431–447 (May 27, 2026)
doi:10.3934/dcdsb.2026078

ANALYSING THE DYNAMICS OF TWO THREE-DIMENSIONAL ODE SYSTEMS DERIVED FROM THE SAME PDE MODEL OF CANCER INVASION

Chloé Colson[*1,2], Philip K. Maini[2] and Faustino Sánchez-Garduño[3]

[1]Centre for Evolution and Cancer, Institute of Cancer Research,
32 Oakleaf Avenue, Sutton, SM2 5GP, UK

[2]Wolfson Centre for Mathematical Biology, Mathematical Institute, University of Oxford,
Radcliffe Observatory Quarter, Oxford, OX2 6GG, UK

[3]Departamento de Matemáticas, Facultad de Ciencias, UNAM, Ciudad Universitaria,
Circuito Exterior, Cd. de México, C.P., 04510, México

(Communicated by King-Yeung Lam)

Abstract. Reaction-diffusion partial differential equations (PDEs) with nonlinear, degenerate diffusion arise in many real-world applications. In this paper, we identify a previously unrecognised feature in the dynamical systems framework typically used to analyse the travelling wave solutions (TWS) of such PDEs: the first-order ordinary differential equation (ODE) system obtained during a travelling wave analysis is not necessarily unique. Using a degenerate-diffusion PDE model of tumour invasion that we have previously studied, we perform the initial steps of a travelling wave analysis and derive two distinct ODE systems. We compare their dynamical properties and show that, although the systems are not topologically equivalent across their entire solution spaces, they are equivalent within the parameter regimes that yield valid TWS of the PDE. Thus, both models can capture the TWS of interest. Importantly, we note that one ODE system is more analytically tractable than the other, demonstrating that the stage at which the standard "desingularisation" step is applied can significantly affect our ability to analyse TWS in PDEs with degenerate diffusion.

1. **Introduction.** Partial differential equation (PDE) models featuring nonlinear degenerate diffusion have been applied to study various real-world systems. This includes the modelling of population dynamics in biology and ecology to describe density-dependent cell migration or organism dispersal [14, 15], porous medium flow in fluid dynamics to describe gas expansion [21] or groundwater infiltration [3], and nonlinear heat conduction in materials such as plasma [2, 23], to name a few.

While such models can admit a great variety of different solution types, much research has focussed on their so-called *travelling wave solutions* (TWS). This is because these solutions have an important physical (in a broad sense) interpretation and they play a fundamental role in both mathematics and mathematical

2020 *Mathematics Subject Classification.* Primary: 37C15, 37M05, 35K57, 35C07; Secondary: 37N25, 35Q92.

Key words and phrases. Cross-degenerate diffusion, travelling wave solutions, 3-d dynamical systems, heteroclinic trajectories, topological equivalence.

*Corresponding author: Chloé Colson.

modelling. Investigations of TWS in one-dimensional space typically touch on two key questions:

1. The existence (and uniqueness) of constant speed, constant profile TWS for a given PDE model and its relevant boundary conditions.
2. The convergence of these TWS: for any wave speed c^* such that $\varphi(x - c^*t)$ is a TWS of the PDE of interest, do other solutions $\Psi(x,t)$ of the PDE, subject to initial conditions with compact support, converge to $\varphi(x-c^*t)$ as $t \to +\infty$, i.e., do we have

$$\lim_{t\to+\infty} |\varphi(x - c^*t) - \Psi(x,t)| = 0?$$

Many approaches have been developed to study the existence of TWS for reaction-diffusion models, from topological methods like the Conley Index or Isolated blocks [4, 9, 11] to singular perturbation methods [10, 19]. Here, we focus on a common dynamical systems approach, which has successfully been applied to prove the existence of TWS and is typically structured as follows [16]. First, spatially homogeneous steady states of the PDE model are identified in order to prescribe boundary conditions for TWS of interest. Then, constant profile, constant speed TWS are sought by introducing a travelling wave coordinate and deriving a nonlinear second-order ordinary differential equation (ODE) model that the TWS must satisfy (assuming a single PDE of second-order in space). After introducing a new dependent variable to obtain a system of first-order ODEs, a local steady state analysis is performed to characterise the ODE model's dynamics near the steady states of interest. Finally, a global analysis is conducted where TWS are defined as heteroclinic trajectories of the ODE system that connect these steady states.

When investigating TWS governed by degenerate diffusion, the second-order ODE (and the first-order ODE system) derived using the above procedure contains a singularity. To simplify the travelling wave analysis, a common approach consists of removing this singularity by re-parametrising the ODE model using a new independent variable (via a homeomorphism, which yields a new ODE system that is orbitally-equivalent to the original system) [1, 7]. This so-called "desingularisation" step can either be performed on the second-order ODE (i.e., before introducing the new dependent variable) [5, 8] or on the equivalent first-order ODE system (i.e., after introducing the new dependent variable) [13, 17, 18, 20].

In this paper, we use a degenerate diffusion PDE model we previously proposed and analysed [5] to show that the first-order ODE system one obtains when performing a travelling wave analysis (as described above) is not necessarily unique. In particular, we derive two distinct ODE systems for our model. We then study the relationship between their dynamics and highlight key implications for proving the existence of TWS. More specifically, we show that the two systems are not necessarily topologically equivalent in their entire solution spaces, with marked differences in the behaviour of the two systems in certain parameter regimes. Crucially, these differences occur between solutions of the two systems which are not valid TWS of the PDE model. Hence, we show that both systems describe the same TWS, despite their differences. However, we also find that the stage at which the desingularisation step is carried out can profoundly impact the analytical tractability of the resulting non-singular system.

PDE model of tumour invasion with nonlinear degenerate diffusion. In previous work [5], we proposed a simple one-dimensional model of tumour invasion

into healthy tissue that describes the interactions between tumour cells and the extracellular matrix (ECM), a scaffold of proteins that holds healthy cells in place and regulates cell signalling [22]. In dimensionless form, the model is given by the following system:

$$\begin{cases} \dfrac{\partial N}{\partial t} = \dfrac{\partial}{\partial x}\left((1-M)\dfrac{\partial N}{\partial x}\right) + (1-N)N, \\ \dfrac{\partial M}{\partial t} = -\kappa N M, \end{cases} \tag{1}$$

where $N(x,t)$ and $M(x,t)$, are the tumour cell and ECM densities, respectively, at position $x \in \mathbb{R}$ and time $t \in (0,+\infty)$, and $\kappa > 0$ is the dimensionless rate of ECM degradation by tumour cells.

We carried out a detailed travelling wave analysis for the system (1) to rigorously prove the existence of two types of TWS. The first type corresponds to the invasion of tumour cells into the ECM, where the ECM is at a maximal density that inhibits all tumour cell movement ahead of the tumour front (i.e., $M = 1$). The second type corresponds to the invasion of tumour cells into the ECM, where the ECM is strictly below its maximal density ahead of the tumour front (i.e., $M < 1$). This distinction is relevant because system (1) is degenerate precisely at $M = 1$. We showed that the first type of TWS exists for all wave speeds $c > 0$, while the second type of TWS exists for wave speeds above a strictly positive minimum speed. This minimum wave speed depends on the dimensionless rate of ECM degradation, κ, such that it is constant for $0 < \kappa < \kappa^*$ and strictly increasing with κ for $\kappa \geq \kappa^*$, where $\kappa^* > 0$ depends on the ECM density ahead of the tumour front.

Paper structure. The remainder of this paper is structured as follows. In section 2, we set up the travelling wave problem previously studied in [5] and derive the two distinct ODE systems that the TWS of system (1) satisfy. In section 3, we characterise the topological equivalence of the two ODE systems and illustrate our analytical findings using numerical simulations in section 4. In section 5, we discuss how both ODE systems are able to describe the same TWS, despite their differences, before concluding with some final remarks in section 6.

2. Obtaining two distinct non-singular ODE systems.

2.1. The travelling wave problem.

To prove the existence of TWS for (1) in [5], we sought constant profile, constant speed TWS by introducing the travelling wave coordinate $\xi = x - ct$. We assumed that the (constant) wave speed $c > 0$ to ensure the tumour invades the ECM from left to right in the spatial domain. Substituting the ansatz $N(x,t) = \mathcal{N}(\xi)$ and $M(x,t) = \mathcal{M}(\xi)$ into the PDE system (1), we found that TWS must satisfy the following ODE system:

$$\begin{cases} \dfrac{\mathrm{d}}{\mathrm{d}\xi}\left((1-\mathcal{M})\dfrac{\mathrm{d}\mathcal{N}}{\mathrm{d}\xi}\right) + c\dfrac{\mathrm{d}\mathcal{N}}{\mathrm{d}\xi} + (1-\mathcal{N})\mathcal{N} = 0, \\ \dfrac{\mathrm{d}\mathcal{M}}{\mathrm{d}\xi} - \dfrac{\kappa}{c}\mathcal{M}\mathcal{N} = 0. \end{cases} \tag{2}$$

In addition, the TWS must connect spatially-homogeneous steady states of the system (1) and we, therefore, required one of the two following sets of asymptotic conditions to be satisfied:

$$\lim_{\xi\to-\infty}(\mathcal{N}(\xi),\mathcal{M}(\xi)) = (1,0), \quad \lim_{\xi\to+\infty}(\mathcal{N}(\xi),\mathcal{M}(\xi)) = (0,1), \tag{3}$$

$$\lim_{\xi\to-\infty}(\mathcal{N}(\xi),\mathcal{M}(\xi))=(1,0),\ \lim_{\xi\to+\infty}(\mathcal{N}(\xi),\mathcal{M}(\xi))=(0,\bar{\mathcal{M}})\text{ with }\bar{\mathcal{M}}\in[0,1). \quad (4)$$

In particular, from a biological perspective, we have that the tumour cell density is at carrying capacity ($\mathcal{N}=1$) and the ECM is fully degraded far behind the wave, while the tumour cell density is zero and the ECM is either at its maximal density ($\mathcal{M}=1$) or at a value $\mathcal{M}\in[0,1)$ far ahead of the wave. As previously mentioned, we distinguished the case where the ECM is at carrying capacity ahead of the wave as the second-order ODE for $\mathcal{N}$ in (2) is singular at $\mathcal{M}=1$. This follows from the PDE for N in (1) being itself degenerate at $M=1$ when the diffusion coefficient $D(M)=1-M$ is zero.

2.2. **Deriving the two ODE systems.** To study TWS that satisfy the asymptotic condition (3) and converge to $(\mathcal{N},\mathcal{M})=(0,1)$ at infinity, we need to elucidate the behaviour of the solutions as their $\mathcal{M}$-component approaches $\mathcal{M}=1$. Since system (2) is singular at $\mathcal{M}=1$, we can apply a standard procedure to remove the singularity, and reparametrise the trajectories of the system by introducing a new independent variable $y=\Phi(\xi)$ defined such that

$$\frac{dy}{d\xi}\equiv\Phi'(\xi)=\frac{1}{1-\mathcal{M}(\xi)}\quad\forall\,\xi\in\mathbb{R}. \quad (5)$$

In addition, to simplify our analysis, we can recast the second-order ODE for $\mathcal{N}$ in (2) into two coupled first-order ODEs by introducing a third dependent variable. These two steps (the desingularisation and the introduction of a new dependent variable) can be completed in two distinct orders:

I. We desingularise system (2) and then introduce the third dependent variable;
II. We introduce a third dependent variable for system (2), and then desingularise the resulting three-dimensional system of first-order ODEs.

In [5], we applied the desingularisation before introducing a third dependent variable (i.e., we followed I). However, as we will now show, the way in which we proceed (I or II) can lead to two distinct three-dimensional ODE systems.

In the first case, we introduce the following dependent variables

$$\mathcal{N}(y)=n_1(\Phi^{-1}(y)),\quad \mathcal{M}(y)=m_1(\Phi^{-1}(y))\quad\forall\,y\in\mathbb{R}. \quad (6)$$

Then, applying the chain rule using (5), we obtain the following desingularised ODE system, for $y\in\mathbb{R}$:

$$\begin{cases}\dfrac{\mathrm{d}^2n_1}{\mathrm{d}y^2}+c\dfrac{\mathrm{d}n_1}{\mathrm{d}y}+(1-n_1)n_1(1-m_1)=0,\\[2ex]\dfrac{\mathrm{d}m_1}{\mathrm{d}y}-\dfrac{\kappa}{c}m_1(1-m_1)n_1=0.\end{cases} \quad (7)$$

By introducing the additional variable $p_1=\frac{\mathrm{d}n_1}{\mathrm{d}y}$ and, using primes to denote derivatives with respect to y, we finally have the system we studied in [5]:

$$\begin{cases}n_1'=p_1,\\ p_1'=-cp_1-(1-n_1)n_1(1-m_1),\\ m_1'=\dfrac{\kappa}{c}m_1(1-m_1)n_1.\end{cases} \quad (8)$$

In the second case, we introduce the variable $\mathcal{P} = \frac{\mathrm{d}\mathcal{N}}{\mathrm{d}\xi}$ into system (2) to obtain the following system of three first order ODEs:

$$\begin{cases} \dfrac{\mathrm{d}\mathcal{N}}{\mathrm{d}\xi} = \mathcal{P}, \\ (1-\mathcal{M})\dfrac{\mathrm{d}\mathcal{P}}{\mathrm{d}\xi} = -\left(c - \dfrac{\kappa}{c}\mathcal{N}\mathcal{M}\right)\mathcal{P} - (1-\mathcal{N})\mathcal{N}, \\ \dfrac{\mathrm{d}\mathcal{M}}{\mathrm{d}\xi} = \dfrac{\kappa}{c}\mathcal{M}\mathcal{N}. \end{cases} \tag{9}$$

Then, to desingularise system (9), we introduce the following dependent variables

$$\mathcal{N}(y) = n_2(\Phi^{-1}(y)), \quad \mathcal{M}(y) = m_2(\Phi^{-1}(y)), \quad \mathcal{P}(y) = p_2(\Phi^{-1}(y)) \quad \forall\, y \in \mathbb{R}. \tag{10}$$

As we did above, applying the chain rule using (5) and, using primes to denote derivatives with respect to y, we obtain the following desingularised system, for $y \in \mathbb{R}$:

$$\begin{cases} n_2' = (1-m_2)p_2, \\ p_2' = -\left(c - \frac{\kappa}{c}n_2 m_2\right)p_2 - (1-n_2)n_2, \\ m_2' = \dfrac{\kappa}{c}m_2(1-m_2)n_2. \end{cases} \tag{11}$$

To be consistent with the asymptotic conditions (3) and (4), we require one of the following to hold, for $i \in \{1,2\}$ and $\bar{m} \in [0,1)$:

$$\lim_{y\to-\infty}(n_i(y),p_i(y),m_i(y)) = (1,0,0), \ \lim_{y\to+\infty}(n_i(y),p_i(y),m_i(y)) = (0,0,1), \tag{12}$$

$$\lim_{y\to-\infty}(n_i(y),p_i(y),m_i(y)) = (1,0,0), \ \lim_{y\to+\infty}(n_i(y),p_i(y),m_i(y)) = (0,0,\bar{m}). \tag{13}$$

In particular, we seek solutions of (8) and (11) that satisfy the same asymptotic conditions (12) and (13). Here, we note that the systems (8) and (11) are clearly defined by different vector fields from $\mathbb{R}^3$ to $\mathbb{R}^3$. Given that we carried out a detailed travelling wave analysis for system (1) in [5] using the ODE system (8), the following questions arise:

1. What is the relationship between the dynamics of systems (8) and (11)?
2. Do the ODE systems (8) and (11) describe the same TWS of the PDE system (1)?
3. Could we perform a similar travelling wave analysis for system (1) using the ODE system (11)?

3. Dynamical relationship between the two ODE systems.

In this section, we investigate the dynamical relationship between systems (8) and (11).

3.1. Two key dynamical concepts.

We begin by introducing two key dynamical concepts.

Definition 3.1 (adapted from [12]). Let $F, G : \Omega \subset \mathbb{R}^n \to \mathbb{R}^n$ be two vector fields. The autonomous ODE systems $\dot{x} = F(x)$ and $\dot{y} = G(y)$, for $x, y \in \Omega$, are called **topologically equivalent** in Ω if there exists a homeomorphism $h : \mathbb{R}^n \to \mathbb{R}^n$ mapping orbits of $\dot{x} = F(x)$ onto orbits of $\dot{y} = G(y)$, preserving the direction of time.

Definition 3.2 (adapted from [12])**.** Let $F, G : \Omega \subset \mathbb{R}^n \to \mathbb{R}^n$ be two vector fields. The autonomous ODE systems $\dot{x} = F(x)$ and $\dot{y} = G(y)$, for $x, y \in \Omega$, are called **smoothly equivalent** in Ω if there exists a diffeomorphism $h : \Omega \to \Omega$ such that, for all $x \in \Omega$,

$$F(x) = M^{-1}(x)G(h(x)), \tag{14}$$

where

$$M(x) = \frac{\mathrm{d}h(x)}{\mathrm{d}x}$$

is the Jacobian matrix of $h(x)$ evaluated at x.

We note here that the key difference between the two types of dynamical equivalence described in Definitions 3.1 and 3.2 is the strength of the requirement on the function h: h is a homeomorphism in Definition 3.1, while h is a diffeomorphism in Definition 3.2. Since any diffeomorphism h is also a homeomorphism, it is straightforward to prove the following result.

Lemma 3.3. *Let $F, G : \Omega \subset \mathbb{R}^n \to \mathbb{R}^n$ be two vector fields. If the autonomous ODE systems $\dot{x} = F(x)$ and $\dot{y} = G(y)$, for $x, y \in \Omega$, are smoothly equivalent in Ω, then they are topologically equivalent in Ω.*

Proof. Let $F, G : \Omega \subset \mathbb{R}^n \to \mathbb{R}^n$ be two vector fields that define two autonomous ODE systems $\dot{x} = F(x)$ and $\dot{y} = G(y)$, for $x, y \in \Omega$. Suppose that these two systems are smoothly equivalent in Ω. Then, Definition 3.2 implies that they can be transformed into each other via the smooth coordinate transformation $y = h(x)$, with h the diffeomorphism in Definition 3.2. This means that there is a homeomorphism h that maps the solutions of $\dot{x} = F(x)$ onto the solutions of $\dot{y} = G(y)$, i.e., h satisfies Definition 3.1 and the two systems are topologically equivalent. □

Note that the reverse implication of Lemma 3.3 is, in general, not true, i.e., two autonomous ODE systems $\dot{x} = F(x)$ and $\dot{y} = G(y)$ that are topologically equivalent in Ω are not necessarily smoothly equivalent in Ω. For example, consider two different two-dimensional ODE systems. Assume that one of them has a steady state that is an asymptotically stable node, i.e., its Jacobian matrix evaluated at the equilibrium has two real negative eigenvalues, and that the second system has a steady state that is an asymptotically stable focus, i.e., its Jacobian matrix evaluated at the equilibrium has two complex eigenvalues with negative real parts. The asymptotically stable node and focus are topologically equivalent, but they are not smoothly equivalent because their respective Jacobian matrices have different eigenvalues (the Jacobians are not similar).

3.2. **The ODE systems are topologically equivalent for $m \in (0, 1)$.** Using the definitions introduced in the previous section, we now show that systems (8) and (11) are topologically equivalent in the region $\mathcal{D} \subset \mathbb{R}^3$, defined as

$$\mathcal{D} = \{(n, p, m) \in \mathbb{R}^3 \,|\, n \in (0, 1),\, p \in (-\infty, 0),\, m \in (0, 1)\}. \tag{15}$$

From our previous travelling wave analysis of system (1) carried out in [5], we know that biologically realistic TWS of (1) remain in region $\mathcal{D}$ for all $y \in \mathbb{R}$. Therefore, region $\mathcal{D}$ is the region of interest for studying TWS of (1).

To prove the topological equivalence of systems (8) and (11) in the region $\mathcal{D}$, we first prove the following lemma:

Lemma 3.4. *The systems (8) and (11) are smoothly equivalent for $(n, p, m) \in \mathcal{D}$.*

Proof. Let us define the function $h : \mathcal{D} \to \mathcal{D}$ as

$$h(n,p,m) := \left(n, \frac{p}{1-m}, m\right). \tag{16}$$

It is straightforward to show that, since $0 < m < 1$ in $\mathcal{D}$, h is smooth and invertible, with its inverse, h^{-1}, itself smooth, in $\mathcal{D}$, i.e., h is a diffeomorphism.

Now, the Jacobian matrix of $h(n,p,m)$ at $(n,p,m) \in \mathcal{D}$ is

$$M = \begin{pmatrix} 1 & 0 & 0 \\ 0 & \frac{1}{1-m} & \frac{p}{(1-m)^2} \\ 0 & 0 & 1 \end{pmatrix}, \tag{17}$$

with inverse

$$M^{-1} = \begin{pmatrix} 1 & 0 & 0 \\ 0 & 1-m & -\frac{p}{(1-m)} \\ 0 & 0 & 1 \end{pmatrix}. \tag{18}$$

We define $S_1, S_2 : \mathcal{D} \to \mathcal{D}$ as $S_1(n_1,p_1,m_1) := (n_1', p_1', m_1')$ and $S_2(n_2,p_2,m_2) := (n_2', p_2', m_2')$, where (n_1', p_1', m_1') and (n_2', p_2', m_2') are, respectively, defined as in (8) and (11). Then, for all $(n_1,p_1,m_1) \in \mathcal{D}$, we have

$$S_2(h(n_1,p_1,m_1)) = \begin{pmatrix} p_1 \\ -\left(c - \frac{\kappa}{c} n_1 m_1\right) \frac{p_1}{1-m_1} - (1-n_1)n_1 \\ \frac{\kappa}{c} m_1(1-m_1)n_1 \end{pmatrix}, \tag{19}$$

and, thus,

$$M^{-1}((n_1,p_1,m_1))S_2(h(n_1,p_1,m_1)) = \begin{pmatrix} p_1 \\ -cp_1 - (1-n_1)n_1(1-m_1) \\ \frac{\kappa}{c} m_1(1-m_1)n_1 \end{pmatrix}. \tag{20}$$

Hence, $S_1(n_1,p_1,m_1) = M^{-1}((n_1,p_1,m_1))S_2(h(n_1,p_1,m_1))$ and, by Definition 3.2, systems (8) and (11) are smoothly equivalent. □

Combining Lemmas 3.3 and 3.4 implies the desired result:

Lemma 3.5. *The systems* (8) *and* (11) *are topologically equivalent for* $(n,p,m) \in \mathcal{D}$.

In fact, one can similarly prove the following, more general result:

Lemma 3.6. *The systems* (8) *and* (11) *are topologically equivalent for* $(n,p,m) \in \Omega$, *where* $\Omega \subset \mathbb{R}^3$ *is defined as*

$$\Omega = \left\{(n,p,m) \in \mathbb{R}^3 \,|\, n \in \mathbb{R},\, p \in \mathbb{R},\, m \in \mathbb{R} \setminus 1\right\}. \tag{21}$$

Importantly, the proof of Lemma 3.6 implies that, by extending the domain (and co-domain) of the homeomorphism h defined in (16) to Ω, h maps solutions of system (8) in Ω to solutions of (11) in Ω.

While the physically-realistic TWS of (1) remain in region $\mathcal{D} \subset \Omega$, we will see that there exist solutions of systems (8) and (11) that leave $\mathcal{D}$, but remain in Ω.

Their topological equivalence outside of $\mathcal{D}$ is relevant to the forthcoming comparison of the two systems' dynamics (see Section 4.3).

3.3. **Breakdown of the ODE systems' topological equivalence at $m = 1$.** In this section, we show that the topological equivalence of systems (8) and (11) at $m = 1$ depends on the dimensionless rate of ECM degradation, κ, and the wave speed, c, leading to a breakdown of their topological equivalence in certain parameter regimes.

It is straightforward to verify that the systems (8) and (11) share the following equilibria:

$$P_0 = (1, 0, 0),\ P_1 = (0, 0, 1),\ P_2 = (1, 0, 1),\ \text{and } P_{\bar{m}} = (0, 0, \bar{m}),\ \bar{m} \in [0, 1). \quad (22)$$

P_0, P_1 and $P_{\bar{m}}$, $\bar{m} \in [0, 1)$, are the biologically-relevant steady states corresponding to spatially homogeneous steady states of system (1). In particular, they are the asymptotic limits of the TWS we seek at $\pm\infty$ defined in (12) and (13).

In addition, the systems (8) and (11) each have another continuum of steady states, with end points at P_1 and P_2. These two continua are not spatially homogeneous equilibria of system (1) and are distinct from one another. They are defined as

$$P^1_{\bar{n}} = (\bar{n}, 0, 1),\ \text{for } \bar{n} \in (0, 1), \quad (23)$$

and

$$P^2_{\bar{n}} = (\bar{n}, p(\bar{n}), 1)\,,\ \text{where } p(\bar{n}) = \frac{\bar{n}(1-\bar{n})}{\frac{\kappa}{c}\bar{n} - c},\ \text{ for } \bar{n} \in (0, 1) \backslash \left\{ \frac{c^2}{\kappa} \right\}, \quad (24)$$

for systems (8) and (11), respectively.

$P^1_{\bar{n}}$ is a straight line segment in the plane $m = 1$, defined for all $\bar{n} \in (0, 1)$ and $\kappa, c > 0$. By contrast, $P^2_{\bar{n}}$ is a curve in the same plane that corresponds to the graph of $p(\bar{n})$, defined in (24), for $\bar{n} \in (0, 1)$. $p(\bar{n})$ is a continuous function for all $\bar{n} \in (0, 1)$ provided $0 < \kappa \leq c^2$ (since this implies that the discontinuity occurs at $\bar{n} = \frac{c^2}{\kappa} \geq 1$) and discontinuous at $\bar{n} = \frac{c^2}{\kappa} \in (0, 1)$, otherwise. In particular, if $\kappa > c^2 > 0$, then $P^2_{\bar{n}}$ is a hyperbola in the plane $m = 1$ with a vertical asymptote at $\bar{n} = \frac{c^2}{\kappa}$, so that $p(\bar{n}) < 0$ for $\bar{n} \in (0, \frac{c^2}{\kappa})$ and $p(\bar{n}) \geq 0$, otherwise.

The change in continuity of $P^2_{\bar{n}}$ that occurs at the threshold value of $\kappa = c^2$ is crucial to the relationship between the dynamics of systems (8) and (11). We find that there is a loss of topological equivalence of the two systems when $m = 1$ if $\kappa > c^2$, while topological equivalence of the two systems appears to be maintained when $\kappa \leq c^2$. We highlight these findings in the following lemma and conjecture. For the purpose of stating our results, let us define a second region $\mathcal{D}' \subset \mathbb{R}^3$ as

$$\mathcal{D}' = \{(n, p, m) \in \mathbb{R}^3 \,|\, n \in (0, 1),\ p \in (-\infty, 0),\ m \in (0, 1]\}. \quad (25)$$

Then, we have the following result.

Lemma 3.7. *If $\kappa > c^2 > 0$, then the systems (8) and (11) are not topologically equivalent for $(n, p, m) \in \mathcal{D}'$.*

Proof. Let $\kappa > c^2 > 0$. Suppose there exists a homeomorphism $h' : \mathcal{D}' \to \mathcal{D}'$ that maps trajectories of system (8) to trajectories of system (11). Then h' also maps fixed points of (8) to fixed points of system (11). Now, we saw above that, when $\kappa > c^2$, $P^1_{\bar{n}}$ is continuous for all $\bar{n} \in (0, 1]$, while $P^2_{\bar{n}}$ has a discontinuity at $\bar{n} = \frac{c^2}{\kappa} \in (0, 1)$. Therefore, there cannot exist a continuous mapping between $P^1_{\bar{n}}$

and $P^2_{\bar{n}}$ for $\bar{n} \in (0,1]$. This implies that h' cannot exist and systems (8) and (11) are not topologically equivalent for $(n,p,m) \in \mathcal{D}'$. □

Now, the function $h : \mathcal{D} \to \mathcal{D}$ given by Equation (16) is not defined at $m = 1$ implying that it is not a homeomorphism on $\mathcal{D}'$. However, numerical simulations of systems (8) and (11) (see Section 4) suggest that h maps steady states $P^1_{\bar{n}}$ to steady states $P^2_{\bar{n}}$ for all $\bar{n} \in (0,1]$ when $0 < \kappa \leq c^2$. We formalise this observation in the following conjecture.

Conjecture 3.8. *If $0 < \kappa \leq c^2$, then the systems (8) and (11) are topologically equivalent for $(n,p,m) \in \mathcal{D}'$.*

In the following section, we support these preceding results by comparing numerical simulations of systems (8) and (11) in different parameter regimes.

4. Numerical comparison of the dynamics of the two ODE systems.

In this section, we present numerical simulations of systems (8) and (11) to compare their dynamics and illustrate the analytical results presented in Section 3.

4.1. Numerical methods.

We solve the systems (8) and (11) numerically for $y \in (y_{-\infty}, y_{+\infty}]$, where $y_{\pm\infty}$ are chosen such that one of the asymptotic conditions (12) or (13) are satisfied, using MATLAB's ODE45 (ODE45 is a single step built-in solver for non-stiff ODEs that is based on an explicit Runge-Kutta (4,5) formula, the Dormand-Prince pair [6]).

According to the asymptotic conditions (12) and (13), we seek TWS which satisfy $\lim_{y\to-\infty}(n_i(y), p_i(y), m_i(y)) = (1,0,0)$ for $i \in \{1,2\}$. Linear stability analyses at the equilibrium point $P_0 = (1,0,0)$ for systems (8) (see [5]) and (11) (result not shown) reveal that, for fixed $c > 0$ and $\kappa > 0$, the solutions of systems (8) and (11) that leave P_0 and remain in region $\mathcal{D}$ must satisfy the following asymptotic conditions as $y \to -\infty$, for any shooting parameter $\alpha \geq 0$ and $i \in \{1,2\}$:

$$\begin{cases} n_i(y) = 1 - e^{\lambda_2 y} + \mathcal{O}(e^{(\lambda_2+\mu)y}), \\ p_i(y) = -\lambda_2 e^{\lambda_2 y} + \mathcal{O}(e^{(\lambda_2+\mu)y}), \\ m_i(y) = \alpha e^{\lambda_3 y} + \mathcal{O}(e^{(\lambda_3+\mu)y}), \end{cases} \tag{26}$$

where

$$\lambda_2 = \frac{-c + \sqrt{c^2+4}}{2}, \ \lambda_3 = \frac{\kappa}{c} \text{ and } \mu = \min(\lambda_2, \lambda_3).$$

When solving the systems (8) and (11), we therefore impose initial conditions given by (26) for $i = 1$ and $i = 2$, respectively.

Remark 4.1. The free parameter α arises because the expression for the unstable manifold at P_0 does not impose any conditions on m_i, and we therefore have a continuum of initial conditions for m_i for $\alpha \geq 0$. As we will observe in the numerical simulations that follow, beyond defining the initial condition for m_i, the choice of α affects how fast solutions of the two ODE systems leave P_0 towards increasing values of m_i and, as a result, determines the value of m_i attained at $y = +\infty$.

4.2. The dynamics of the ODE systems when $\kappa \leq c^2$.

In this section, we illustrate the hypothesised topological equivalence of ODE systems (8) and (11) in region $\mathcal{D}'$ provided $0 < \kappa \leq c^2$ (Conjecture 3.8) using representative numerical simulations.

Figures 1 and 2 compare the solutions of systems (8) and (11), subject to initial conditions (26) with increasing α, for $c^2 = 4 > 1 = \kappa$. We first observe that the two

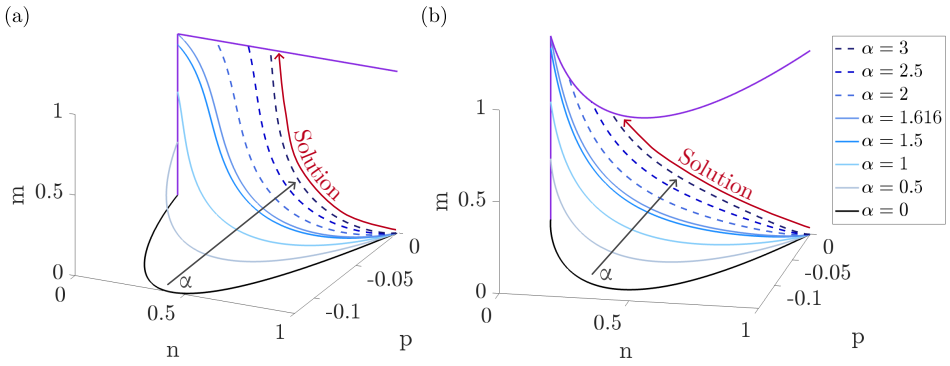

FIGURE 1. Phase space of systems (8) (a) and (11) (b) subject to the asymptotic conditions (26) for $\alpha \in \{0, 0.5, 1, 1.5, 1.616, 2, 2.5, 3\}$, $\kappa = 1$ and $c = 2$ (hence $c^2 > \kappa$). The purple lines represent the two continua of equilibria of each system, i.e., $P_{\bar{m}}$ (a)-(b), and $P^1_{\bar{n}}$ (a) or $P^2_{\bar{n}}$ (b), defined in Equations (22), (23) and (24), respectively. Since the spatially homogeneous steady states of (1) correspond to $(n, m) = (0, \bar{m})$, $\bar{m} \in [0, 1]$ and $(n, m) = (1, 0)$, the dashed curves represent solutions that are not TWS of system (1). The black arrow shows the evolution of trajectories for increasing values of α, and the red, curved arrow represents the direction of the trajectories that leave $(n, p, m) = (1, 0, 0)$. The n and m components of the trajectory are equal for both systems (see Figure 2), and the values m and n attain at infinity increase monotonically (between 0 and 1) with α for both systems.

systems' qualitative behaviour is the same for all values of α. In particular, the n- and m-components of both systems' solutions are strictly monotonic functions of $y \in \mathbb{R} \cup \{-\infty, +\infty\}$, and the values of n and m attained at infinity, $n_{+\infty}$ and $m_{+\infty}$, respectively, increase as α increases. Furthermore, there exists a unique threshold value of α, say α_1, which depends on c and κ [5] (here, $\alpha_1 \approx 1.616$), such that:

- If $\alpha < \alpha_1$, then $n_{+\infty} = 0$ and $m_{+\infty} \in [0, 1)$.
- If $\alpha = \alpha_1$, then $n_{+\infty} = 0$ and $m_{+\infty} = 1$.
- If $\alpha > \alpha_1$, then $n_{+\infty} \in (0, 1]$ and $m_{+\infty} = 1$.

Figure 2 further shows that we also have quantitative agreement between the n- and m-components of both systems' solutions for all values of α considered, i.e., $n_1(y) = n_2(y)$ and $m_1(y) = m_2(y)$ for all $y \in \mathbb{R} \cup \{-\infty, +\infty\}$. In addition, we have $p_1(y) = p_2(y)(1 - m_2(y))$ for all $y \in \mathbb{R} \cup \{-\infty, +\infty\}$. In other words, letting h be the homeomorphism defined in (16), then $h^{-1}(n_2, p_2, m_2) = (n_1, p_1, m_1)$ for all $y \in \mathbb{R} \cup \{-\infty, +\infty\}$, and h maps trajectories of system (8) into the trajectories of system (11).

These results support the topological equivalence of both systems in region $\mathcal{D}'$ when $c^2 > \kappa$.

Remark 4.2. From our previous work [5], we know that, if $c \geq 2$ and $\kappa > 0$, then, for all $\alpha \geq 0$, the solution of system (8) subject to the asymptotic conditions (26) remains in region $\mathcal{D}$ (defined in (15)) for all $y \in \mathbb{R}$, i.e., there are no oscillatory

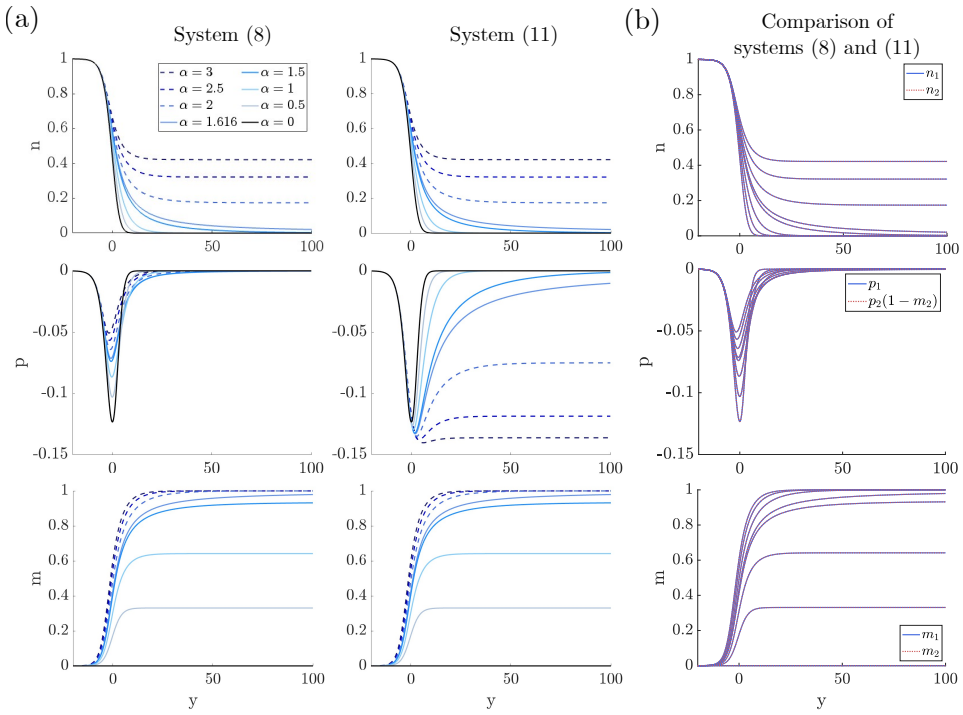

FIGURE 2. We solve systems (8) and (11) for $y \in (-20, 1000]$ subject to initial conditions (26) for $\alpha \in \{0, 0.5, 1, 1.5, 1.616, 2, 2.5, 3\}$, $\kappa = 1$ and $c = 2$ (hence $c^2 > \kappa$). In (a), we plot the components $n_i(y)$, $p_i(y)$, and $m_i(y)$, $i = 1, 2$, of the corresponding solutions for $y \in [-20, 100]$. In (b), we superimpose $n_1(y)$, $p_1(y)$ and $m_1(y)$, and $n_2(y)$, $p_2(y)(1 - m_2(y))$ and $m_2(y)$ for $y \in [-20, 100]$. We observe that $n_1(y) = n_2(y)$, $p_1(y) = p_2(y)(1 - m_2(y))$ and $m_1(y) = m_2(y)$ for $y \in [-20, 100]$. This shows how the homeomorphism h defined by (16) maps trajectories of system (8) to trajectories of system (11).

dynamics about fixed points. By the topological equivalence of systems (8) and (11), this also holds for the solutions of system (11) subject to the asymptotic conditions (26).

4.3. **The dynamics of the ODE systems when $\kappa > c^2$.** In this section, we use representative numerical simulations to show that the ODE systems (8) and (11) are not topologically equivalent in region $\mathcal{D}'$ when $\kappa > c^2$, as stated in Lemma 3.7.

Figures 3 and 4 compare the solutions of systems (8) and (11), subject to initial conditions (26) with increasing α, for $\kappa = 1 > 0.25 = c^2$. In contrast to the previous case, the two systems' qualitative behaviour agrees only for sufficiently small values of α (i.e., $\alpha \leq 30$), with significant differences observed for large values of α (i.e., $\alpha \geq 50$).

Where both systems agree, there exists a threshold value of α, say α_m^* (here, $15 \leq \alpha_m^* < 22.6$), such that, for all $\alpha \in [0, \alpha_m^*]$, there are oscillatory dynamics around the fixed points $P_{\bar{m}} = (0, 0, \bar{m})$ for any $\bar{m} \in [0, m^*(c, \kappa)] \subset [0, 1)$. $m^*(c, \kappa)$ is

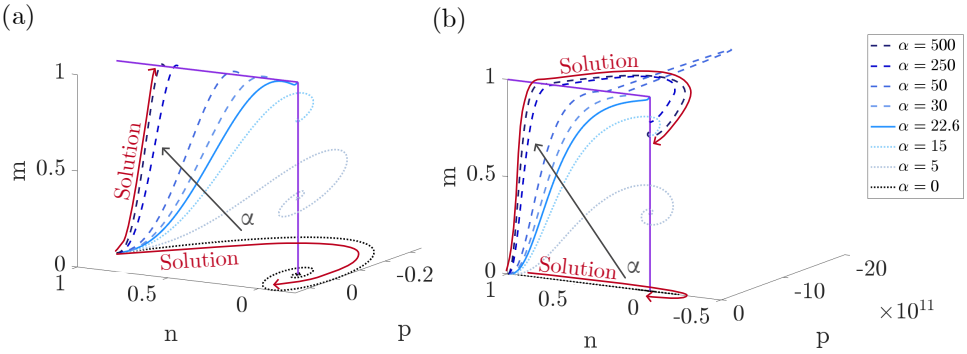

FIGURE 3. Solutions (n, p, m) of systems (8) and (11) subject to the asymptotic conditions (26) for $\alpha \in \{0, 5, 15, 22.6, 50, 250, 500, 1000\}$, $\kappa = 1$ and $c = 0.5$ (hence $c^2 < \kappa$). The purple lines represent the two continua of equilibria of each system, i.e., $P_{\bar{m}}$ (a)-(b), and $P^1_{\bar{n}}$ (a) or $P^2_{\bar{n}}$ (b), defined in Equations (22), (23) and (24), respectively, with only equilibria on $P^2_{\bar{n}}$ with negative p-component shown in (b). Since the spatially homogeneous steady states of (1) correspond to $(n, m) = (0, \bar{m})$, $\bar{m} \in [0, 1]$ and $(n, m) = (1, 0)$, the dashed curves represent solutions that are not TWS of system (1). The dotted curves represent physically unrealistic solutions of system (1) for which the n-component becomes negative; these solutions are also not TWS of system (1) as solutions of system (1) subject to non-negative initial conditions remain non-negative for all time. The black arrow shows the evolution of trajectories for increasing values of α, and the red, curved arrow represents the direction of the trajectories that leave $(n, p, m) = (1, 0, 0)$. The n and m components of the trajectory no longer agree for both systems for all values of α (see Figure 4). The values m and n attain at infinity increase monotonically (between 0 and 1) with α for system (8), whereas they are monotonically increasing for $\alpha \leq 30$ and monotonically decreasing for $\alpha \geq 50$ for system (11).

the threshold value of $\bar{m}$ (that corresponds to α^*_m) below which solutions of (8) that satisfy the asymptotic conditions (26) and converge to $(0, 0, \bar{m})$ as $y \to +\infty$ leave region $\mathcal{D}$ for some $y \in \mathbb{R}$ (as the n-component of the solution becomes negative). We proved the existence of α^*_m and the corresponding $m^*(c, \kappa)$ for system (8) in [5]. Lemma 3.6 implies that these threshold values exist and are the same for system (11), as illustrated in Figures 3 and 4.

Now, as proved in our previous work [5] and illustrated in Figures 3 and 4, the solutions of system (8) that satisfy the asymptotic conditions (26), with $\alpha > \alpha^*_m$ (i.e., $\alpha \geq 22.6$), remain in region $\mathcal{D}$ for all $y \in \mathbb{R}$. The n- and m-components of such solutions are strictly monotonic functions of $y \in \mathbb{R} \cup \{-\infty, +\infty\}$, and $n_{+\infty}$ and $m_{+\infty}$ increase as α increases. As for the case when $0 \leq \kappa \leq c^2$, there exists $\alpha_1 > \alpha^*_m$ (here, $\alpha_1 \approx 22.6$) such that:

- If $\alpha^*_m < \alpha < \alpha_1$, then $n_{+\infty} = 0$ and $m_{+\infty} \in (m^*(c, \kappa), 1)$.
- If $\alpha = \alpha_1$, then $n_{+\infty} = 0$ and $m_{+\infty} = 1$.

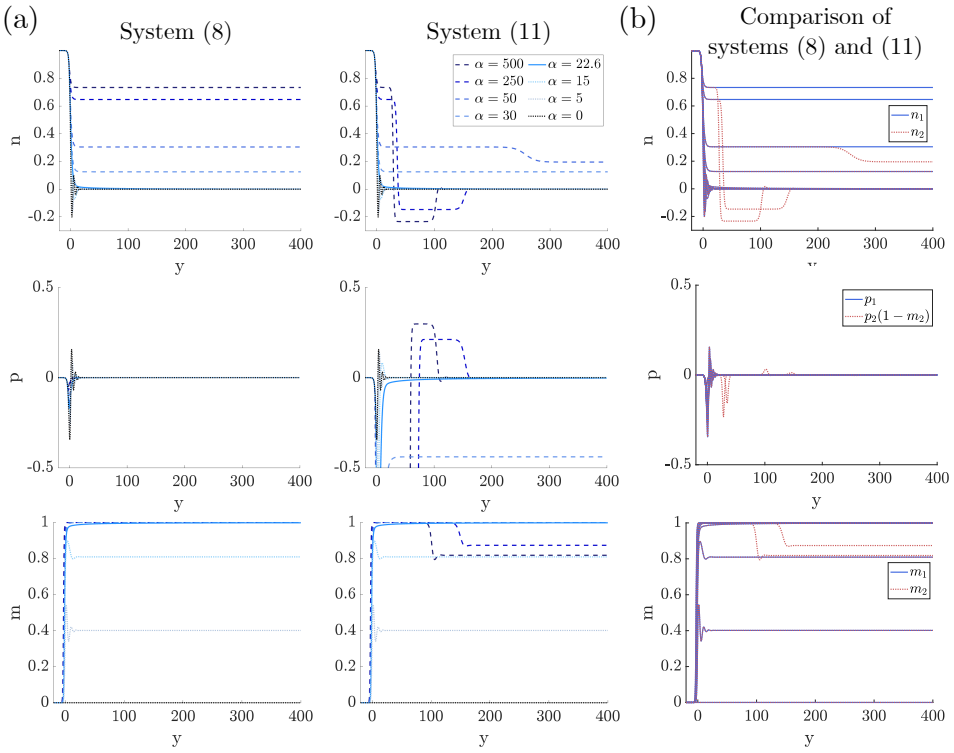

FIGURE 4. We solve systems (8) and (11) for $y \in (-20, 1000]$ subject to initial conditions (26) for $\alpha \in \{0, 5, 15, 22.6, 30, 50, 250, 500\}$, $\kappa = 1$ and $c = 0.5$ (hence $c^2 < \kappa$). In (a), we plot the components $n_i(y)$, $p_i(y)$, and $m_i(y)$, $i = 1, 2$, of the corresponding solutions for $y \in [-20, 400]$. In (b), we plot $n_1(y)$, $p_1(y)$ and $m_1(y)$, and $n_2(y)$, $p_2(y)(1 - m_2(y))$ and $m_2(y)$ for $y \in [-20, 400]$. We observe that, for $\alpha \leq 30$, $n_1(y) = n_2(y)$ and $m_1(y) = m_2(y)$ for all $y \in [-20, 400]$, while values of $\alpha \geq 50$ are associated with significant differences between $n_1(y)$ and $n_2(y)$, and $m_1(y)$ and $m_2(y)$. Consistently, $p_1(y) = p_2(y)(1-m_2(y))$ for all $y \in [-20, 400]$ when $\alpha \leq 30$, whereas there exist $y \in [-20, 400]$ such that $p_1(y) \neq p_2(y)(1 - m_2(y))$ when $\alpha \leq 50$. This shows how the homeomorphism h defined by (16) does not map all trajectories of system (8) to all trajectories of system (11).

- If $\alpha > \alpha_1$, then $n_{+\infty} \in (0, 1]$ and $m_{+\infty} = 1$.

Comparing the solutions of system (11) to those of system (8) when $\alpha \geq 22.6$, we note that there exists a threshold value of $\alpha > \alpha_1$, say $\bar{\alpha}$ (here, $30 < \bar{\alpha} \leq 50$), such that:

- If $\alpha_m^* < \alpha \leq \bar{\alpha}$, then the solutions of system (11) have the same qualitative behaviour as the solutions of system (8) (see the above description).
- If $\alpha > \bar{\alpha}$, then the solutions of system (11) that satisfy the asymptotic conditions (26) may leave region $\mathcal{D}$ for some $y \in \mathbb{R}$ (as the n-component of the solution becomes negative). In that case, the n- and m-components of such

solutions are non-monotonic, oscillatory functions of $y \in \mathbb{R} \cup \{-\infty, +\infty\}$. In addition, even if the solution remains in region $\mathcal{D}$ for all $y \in \mathbb{R}$ (e.g., $\alpha = 50$ in Figures 3 and 4), the values of $n_{+\infty}$ and $m_{+\infty}$ decrease as α increases from $\bar{\alpha}$.

In particular, while the solutions of (8) are monotonic with respect to $\alpha \geq 0$, the solutions of (11) are not.

Consistent with these observations, Figure 4 further shows that, when $\alpha \leq 30$, there is quantitative agreement between the n- and m-components of both systems' solutions (i.e., $n_1(y) = n_2(y)$ and $m_1(y) = m_2(y)$ for all $y \in \mathbb{R} \cup \{-\infty, +\infty\}$) and we also have that $p_1(y) = p_2(y)(1 - m_2(y))$ for all $y \in \mathbb{R} \cup \{-\infty, +\infty\}$. However, these equalities no longer hold when $\alpha \geq 50$. Indeed, when $\alpha \geq 50$, the solutions of systems (8) and (11) reach the plane $m \equiv 1$ for some $\bar{y} \in \mathbb{R}$. At this point, $(n_1(\bar{y}), p_1(\bar{y}), m_1(\bar{y})) = (\bar{n}_1, 0, 1) \in P^1_{\bar{n}}$ (defined in Equation (23)), which is a steady state of (8). By contrast, $(n_2(\bar{y}), p_2(\bar{y}), m_2(\bar{y})) = (\bar{n}_2, \bar{p}_2, 1) \notin P^2_{\bar{n}}$ (defined in Equation (24)), which is not a steady state of (11) because $\bar{n}_2 \geq c^2/\kappa = 0.25$ and $\bar{p}_2 < 0$, but the steady state value of p that corresponds to $\bar{n}_2$, defined in Equation (24), satisfies $p(\bar{n}_2) \geq 0$. Thus, while $(n_1(\bar{y}), p_1(\bar{y}), m_1(\bar{y})) \equiv (\bar{n}_1, 0, 1)$ for all $y \geq \bar{y}$, for system (11) to reach a valid steady state, the solution continues to evolve until it reaches a steady state with $n \in [0, 1]$, $m \in [0, 1]$ and $p = p(n)$ defined in Equation (24).

Note that this result does not contradict the topological equivalence of the two systems in region $\mathcal{D}$ (Lemma 3.5). Indeed, since $\mathcal{D}$ does not include the plane $m \equiv 1$, we only expect the homeomorphism h defined in (16) to map trajectories of system (8) onto the trajectories of system (11) for $y \in (-\infty, \bar{y})$.

We observe the preceding behaviour across a range of values of κ, $c > 0$ such that $\kappa > c^2$ (results not shown). In particular, in each case, we find that there exists a threshold value $\bar{\alpha}(c, \kappa) > \alpha_1(c, \kappa)$ above which solutions of system (11) lose their monotonicity with respect to α (results not shown). The existence of such an $\bar{\alpha}(c, \kappa)$ is an indicator that systems (8) and (11) are not topologically equivalent in region $\mathcal{D}'$.

Remark 4.3. Our numerical simulations suggest that the threshold value of α, $\bar{\alpha}(c, \kappa)$, above which we observe discrepancies between the solutions of systems (8) and (11) is strictly greater than $\alpha_1(c, \kappa)$, the unique value of α such that the solutions converge to $(n, p, m) = (0, 0, 1)$ as $y \to +\infty$. We can prove that this must be the case by recalling (from [5]) that $\alpha_1(c, \kappa)$ exists for all $c > 0$ and $\kappa > 0$, and that the solution of (8) that satisfies the asymptotic conditions (26) for $\alpha = \alpha_1(c, \kappa)$ remains in region $\mathcal{D}$ for all $y \in \mathbb{R}$ and converges to $(0, 0, 1)$ as $y \to +\infty$. Hence, we can use the homeomorphism h defined by (16) to map this solution of system (8) to a solution of system (11) defined for all $y \in \mathbb{R}$. Since $n_2(y) = n_1(y)$ and $m_2(y) = m_1(y)$ for all $y \in \mathbb{R}$ (according to h), the convergence (as $y \to +\infty$) and continuity of both systems' solutions imply that the solution of system (11) must also converge to $(0, 0, 1)$ as $y \to +\infty$. As a result, there is no discrepancy between the solutions of both systems for $\alpha = \alpha_1$ and we must have $\bar{\alpha}(c, \kappa) > \alpha_1$. This argument reappears in the following section, where we show that both systems describe the same TWS of system (1).

5. Both ODE systems describe the same travelling wave solutions of PDE model (1).

In our previous work [5], we proved that, given $\kappa > 0$, for any $\bar{M} \in [0, 1)$, there exists a minimum wave speed, $c_\kappa(\bar{M})$, such that:

1. For $c < c_\kappa(\bar{M})$, system (1) has no TWS connecting $(N, M) = (1, 0)$ and $(N, M) = (0, \bar{M})$.
2. For $c \geq c_\kappa(\bar{M})$, system (1) has a smooth TWS connecting $(N, M) = (1, 0)$ and $(N, M) = (0, \bar{M})$. This solution is unique (up to translation) and N, M are monotonically decreasing and increasing functions of $x - ct = \xi \in \mathbb{R} \cup \{-\infty, +\infty\}$, respectively.

We also proved that, given $\kappa > 0$ and $\bar{M} = 1$, system (1) has a smooth TWS connecting $(N, M) = (1, 0)$ and $(N, M) = (0, 1)$ for any $c > 0$. This solution is unique (up to translation) and N, M are monotonically decreasing and increasing functions of $x - ct = \xi \in \mathbb{R} \cup \{-\infty, +\infty\}$, respectively.

In order to prove these results, we showed that, if $\kappa > 0$ and $\bar{M} \in [0, 1)$ $(\bar{M} = 1)$, then, for any $c \geq c_\kappa(\bar{M})$ $(c > 0)$, there exists a unique value of the shooting parameter $\alpha(c) \geq 0$ (defined in (26)) such that the solution $(n_1(y), p_1(y), m_1(y))$ of system (8) that satisfies the asymptotic conditions (26) remains in region $\mathcal{D}$ for all $y \in \mathbb{R}$ and converges to $(0, 0, \bar{M})$ as $y \to +\infty$. We then constructed the smooth TWS of system (1) connecting $(N, M) = (1, 0)$ and $(N, M) = (0, \bar{M})$ using this solution by setting $(\mathcal{N}_1(\xi), \mathcal{M}_1(\xi)) := (n_1(\Phi(\xi)), m_1(\Phi(\xi))$, where Φ is defined in (5).

Let $\kappa > 0$, $\bar{M} \in [0, 1)$ $(\bar{M} = 1)$ and $c \geq c_\kappa(\bar{M})$ $(c > 0)$. We now show that we can construct the same smooth TWS of system (1) connecting $(N, M) = (1, 0)$ and $(N, M) = (0, \bar{M})$ from a solution of system (11).

Fix $\alpha = \alpha(c)$ such that the solution $(n_1(y), p_1(y), m_1(y))$ of system (8) that satisfies the asymptotic conditions (26) remains in region $\mathcal{D}$ for all $y \in \mathbb{R}$ and converges to $(0, 0, \bar{M})$ as $y \to +\infty$. Let $(n_2(y), p_2(y), m_2(y))$ be the solution of (11) that satisfies the asymptotic conditions (26) for the same α.

In Sections 3 and 4, we showed the topological equivalence of systems (8) and (11) in region $\mathcal{D}$ for all $c > 0$ and $\kappa > 0$. Using the homeomorphism h, defined in (16), that maps solutions of system (8) to solutions of system (11) in region $\mathcal{D}$, we know that $(n_2(y), m_2(y)) = h(n_1(y), m_1(y)) = (n_1(y), m_1(y))$ for all $y \in \mathbb{R} \cup \{-\infty\}$. By the convergence (as $y \to +\infty$) and continuity of solutions of systems (8) and (11), it is straightforward to show that $\lim_{y\to+\infty}(n_2(y), m_2(y)) = \lim_{y\to+\infty} h(n_1(y), m_1(y)) = (0, \bar{M})$.

We can then set

$$\begin{aligned}(\mathcal{N}_2(\xi), \mathcal{M}_2(\xi)) &:= (n_2(\Phi(\xi)), m_2(\Phi(\xi)) \\ &= (n_1(\Phi(\xi)), m_1(\Phi(\xi)) \\ &=: (\mathcal{N}_1(\xi), \mathcal{M}_1(\xi))\end{aligned} \tag{27}$$

for all $\xi \in \mathbb{R} \cup \{-\infty, +\infty\}$, where Φ is defined in (5).

Hence, the solution $(n_2(y), p_2(y), m_2(y))$ of system (11) can be used to construct solutions $(\mathcal{N}_2(\xi), \mathcal{M}_2(\xi))$, $\xi \in \mathbb{R} \cup \{-\infty, +\infty\}$, that are equal to the TWS, $(\mathcal{N}_1(\xi), \mathcal{M}_1(\xi))$, $\xi \in \mathbb{R} \cup \{-\infty, +\infty\}$, of the PDE model (1) constructed using system (8).

Overall, we have proved that, for any $c > 0$ and $\kappa > 0$, the systems (8) and (11) describe the same TWS, despite the fact that the two systems are not topologically equivalent in the plane $m \equiv 1$.

6. **Concluding remarks.** In this paper, we considered a reaction-diffusion PDE model of tumour invasion (1) characterised by nonlinear, degenerate cross-diffusion. We previously carried out a travelling wave analysis for this model in [5] using an ODE system that was derived by applying a classical desingularisation procedure

and, subsequently, introducing an additional dependent variable to obtain a first-order system. One might assume that such an ODE system is unique for any given PDE system. However, we found that another, different ODE system can also be derived from system (1) if we switch the ordering of the desingularisation and the introduction of the new dependent variable. Our aim here was, therefore, to investigate the dynamical relationship between the two distinct ODE systems that correspond to PDE system (1), in particular, in the context of its TWS.

Accordingly, we derived the two distinct ODE systems, (8) and (11), and showed analytically and numerically that, while both of these systems describe the same TWS of (1), they are not always topologically equivalent in the systems' solution spaces. In particular, their topological equivalence is parameter-dependent and only guaranteed when $0 \leq \kappa \leq c^2$, where we recall that κ is the dimensionless ECM degradation rate and c is the wave speed. When $\kappa > c^2$, we no longer have topological equivalence in the plane $m \equiv 1$, which leads to the breakdown in topological equivalence of the two systems.

The lack of topological equivalence of systems (8) and (11) when $\kappa > c^2$ is of particular interest because it is associated with the solutions of system (11) no longer being monotonic with respect to the shooting parameter $\alpha \geq 0$. Indeed, the monotonicity of solutions with respect to α is a key property satisfied by system (8) for all $c > 0$ and $\kappa > 0$. Without this desirable property, the proof of the existence and uniqueness of TWS of system (1) that we developed in [5] breaks down. In other words, our proof could not have been applied to system (11), and a different approach would be necessary using this second system.

This present study, thus, highlights the importance of carefully considering when to apply a desingularisation procedure when studying TWS of degenerate PDE models. The timing of the desingularisation step can lead to distinct ODE systems that may have more or less desirable properties depending on the intended goal of the study. In general, applying the desingularisation step such that the resulting ODE system is non-singular (i.e., as system (8) and unlike system (9)) is likely to be the more appropriate approach.

Acknowledgments. We thank Helen M. Byrne and Tommaso Lorenzi for helpful discussions.

REFERENCES

[1] D. G. Aronson, Density-dependent interaction–diffusion systems, *Dynamics and Modelling of Reactive Systems*, Academic Press, New York, (1980), 161-176.

[2] D. G. Aronson, The porous medium equation, *Nonlinear Diffusion Problems: Lectures Given at the 2nd 1985 Session of the Centro Internazionale Matermatico Estivo (CIME) held at Montecatini Terme*, Berlin, (2006), 1-46.

[3] J. Bear and A. H.-D. Cheng, *Modeling Groundwater Flow and Contaminant Transport*, Springer, 2010.

[4] C. Conley and R. Gardner, An application of the generalized Morse index to travelling wave solutions of a competitive reaction-diffusion model, *Indiana Univ. Math. J.*, **33** (1984), 319-343.

[5] C. Colson, F. Sánchez-Garduño, H. M. Byrne, P. K. Maini and T. Lorenzi, Travelling-wave analysis of a model of tumour invasion with degenerate, cross-dependent diffusion, *Proc. R. Soc. A: Math. Phys. Eng. Sci.*, **477** (2021).

[6] J. R. Dormand and P. J. Prince, A family of embedded Runge-Kutta formulae, *J. Comput. Appl. Math*, **6** (1980), 19-26.
[7] H. Engler, Relations between travelling wave solutions of quasilinear parabolic equations, *Proc. Amer. Math. Soc.*, **93** (1985), 297-302.
[8] T. Gallay and C. Mascia, Propagation fronts in a simplified model of tumor growth with degenerate cross-dependent self-diffusivity, *Nonlinear Anal. Real World Appl.*, **63** (2022).
[9] R. A. Gardner, Existence of travelling wave solutions of predator–prey systems via the connection index, *SIAM J. Appl. Math.*, **44** (1984), 56-79.
[10] K. Harley, P. van Heijster, R. Marangell, G. J. Pettet and M. Wechselberger, Existence of traveling wave solutions for a model of tumor invasion, *SIAM J. Appl. Dyn. Syst.*, **13** (2014), 366-396.
[11] B. Kaźmierczak, Existence of travelling wave solutions for reaction-diffusion-convection systems via the Conley index theory, *Topol. Methods Nonlinear Anal.*, **17** (2001), 359-403.
[12] Y. A. Kuznetsov, *Elements of Applied Bifurcation Theory*, NY: Springer New York, 1998.
[13] L. Malaguti and C. Marcelli, Sharp profiles in degenerate and doubly degenerate Fisher-KPP equations, *J. Differ. Equ.*, **195** (2003), 471-496.
[14] J. D. Murray, *Mathematical Biology: II: Spatial Models and Biomedical Applications*, NY: Springer New York, 2003.
[15] B. Perthame, *Parabolic Equations in Biology: Growth, Reaction, Movement and Diffusion*, Cham: Springer International Publishing, 2015.
[16] F. Sánchez-Garduño and V. Castellanos, Traveling wave solutions for nonlinear reaction-diffusion equations as dynamical systems problems, *Lobachevskii J. Math.*, **43** (2022), 141-161.
[17] F. Sánchez-Garduño and P. K. Maini, Travelling wave phenomena in non-linear diffusion degenerate Nagumo equations, *J. Math. Biol.*, **35** (1997), 713-728.
[18] F. Sánchez-Garduño, P. K. Maini and M. E. Kappos, A shooting argument approach to a sharp-type solution for nonlinear degenerate Fisher-KPP equations, *IMA J. Appl. Math.*, **57** (1996), 211-221.
[19] J. Sherratt, On the form of smooth-front travelling waves in a reaction-diffusion equation with degenerate nonlinear diffusion, *Math. Model. Nat. Phenom.*, **5** (2010), 64-79.
[20] M. J. Simpson and S. W. McCue, Fisher–KPP-type models of biological invasion: Open source computational tools, key concepts and analysis, *Proc. R. Soc. A: Math. Phys. Eng. Sci.*, **480** (2024).
[21] J. L. Vázquez, *The Porous Medium Equation: Mathematical Theory*, Clarendon Press, 2006.
[22] Z. Werb, ECM and cell surface proteolysis: Regulating cellular ecology, *Cell*, **91** (1997), 439-442.
[23] Y. B. Zel'dovich and Y. P. Raizer, *Physics of Shock Waves and High–Temperature Hydrodynamic Phenomena*, Courier Corporation, 2002.

Received for publication January 13, 2026; early access May 27, 2026.